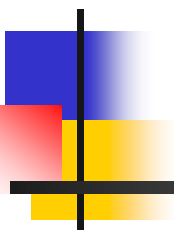


Cosmic Polarization Rotation (CPR) induced
from Pseudoscalar-Photon interaction
and
New CPR Constraints from BICEP2 & SPTpol
Detections of CMB B-Mode Polarization



Wei-Tou Ni

Department of Physics

National Tsing Hua University

Hsinchu, Taiwan, ROC

[1] W.-T. Ni, Reports on Progress in Physics, 73, 056901 (2010).

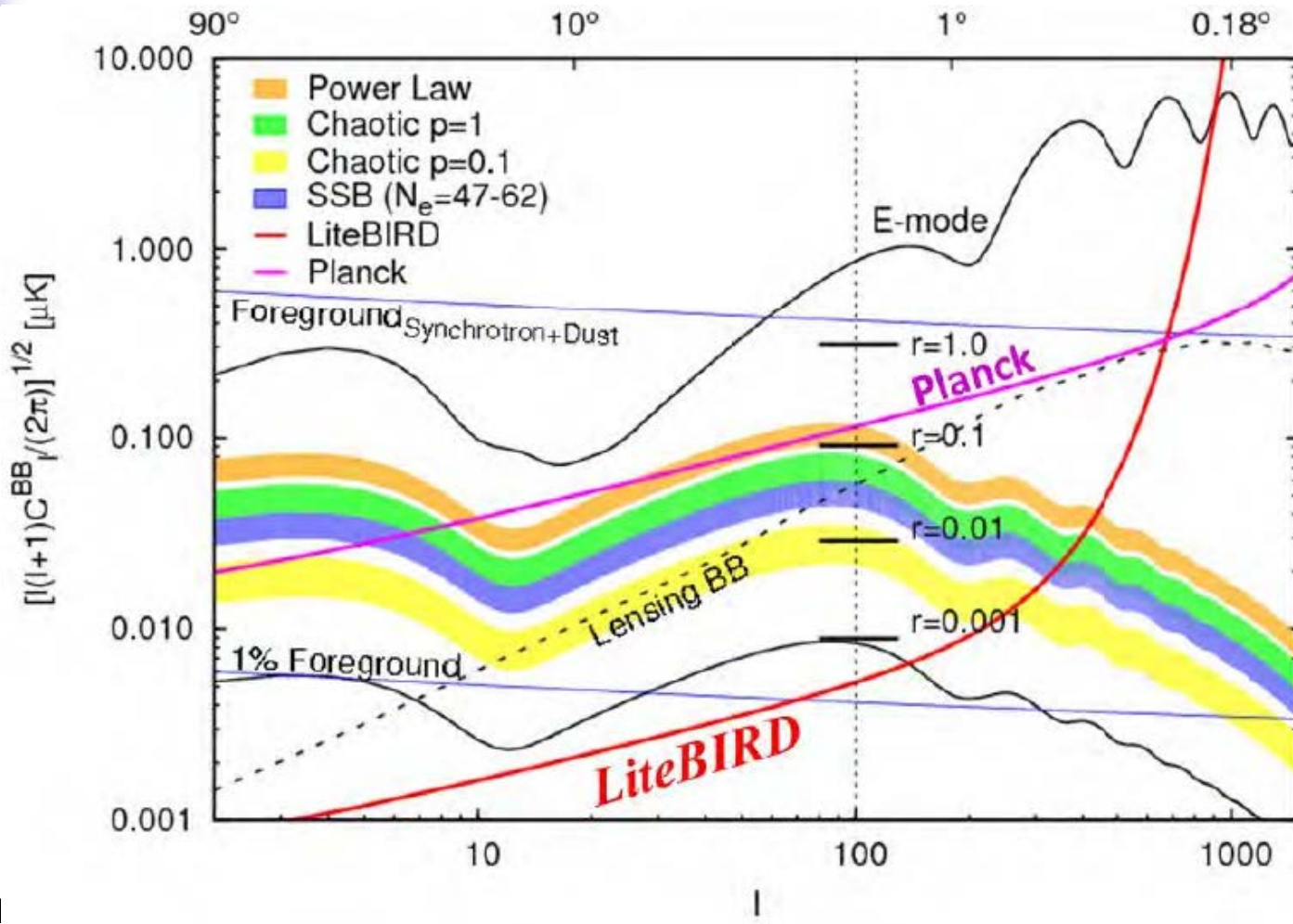
[2] Sperello di Serego Alighieri, Wei-Tou Ni and Wei-Ping Pan, arXiv:1404.1701 (2014).

Introduction – CMB observations

7 orders or more improvement in amplitude,
15 orders improvement in power since 1965

- **1948** Gamow – hot big bang theory; Alpher & Hermann – about 5 K CMB
- Dicke -- oscillating (recycling) universe: entropy → CMB
- **1965** Penzias-Wilson excess antenna temperature at 4.08 GHz 3.5 ± 1 K 2.5 → 4.5 (CMB temperature measurement)
- Precision to $10^{-(3-4)}$ → dipolar (earth) velocity measurement
- to $10^{-(5-6)}$ **1992** COBE anisotropy meas. → acoustic osc.
- **2002** Polarization measurement (DASI)
- **2013** Lensing B-mode polarization (SPTpol)
- **2014** Indication of Primitive *Tensor B-mode* (r) (BICEP2)

Example sensitivity goals at 2008: Litebird



The cosmic microwave background radiation temperature at a redshift of 2.34 Present & Past

R. Srianand^{*}, P. Petitjean^{†‡} & C. Ledoux[§]

^{*} IUCAA, Post Bag 4, Ganeshkhind, Pune 411 007, India

[†] Institut d'Astrophysique de Paris-CNRS, 98bis Boulevard Arago, F-75014 Paris, France

[‡] CNRS 173-DAEC, Observatoire de Paris-Meudon, F-92195 Meudon Cedex, France

[§] European Southern Observatory, Karl Schwarzschild Strasse 2, D-85748 Garching bei München, Germany

$$T(\bar{z}) = T(\bar{z} = 0)(1 + z)$$

- $6.0\text{K} < T(2.33771) < 14\text{K}$ Prediction: $9.1\text{ K}(2000)$
- The measurement is based on the excitation of the two first hyperfine levels of carbon (C and C+ induced by collisions and by the tail of the CMB photon distributions. Nature 2000 (inconsistency : H2 and HD abundance measurement) (2001)
- The cosmic microwave background radiation temperature at $z = 3.025$ toward QSO0347-3819, P Molaro et al Astronomy & Astrophysics 2002
- Measurement of effective temperature at different redshift

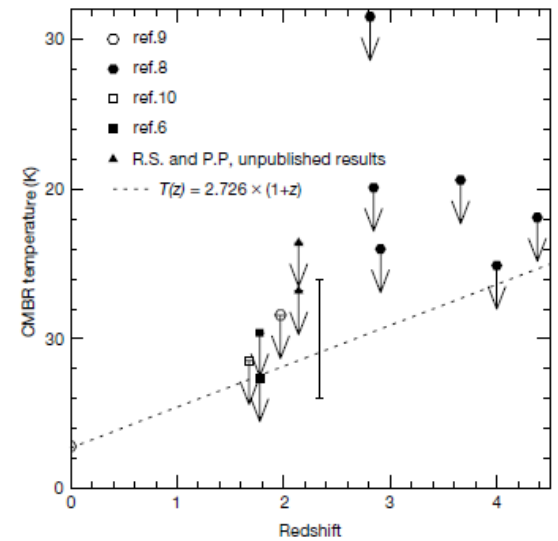
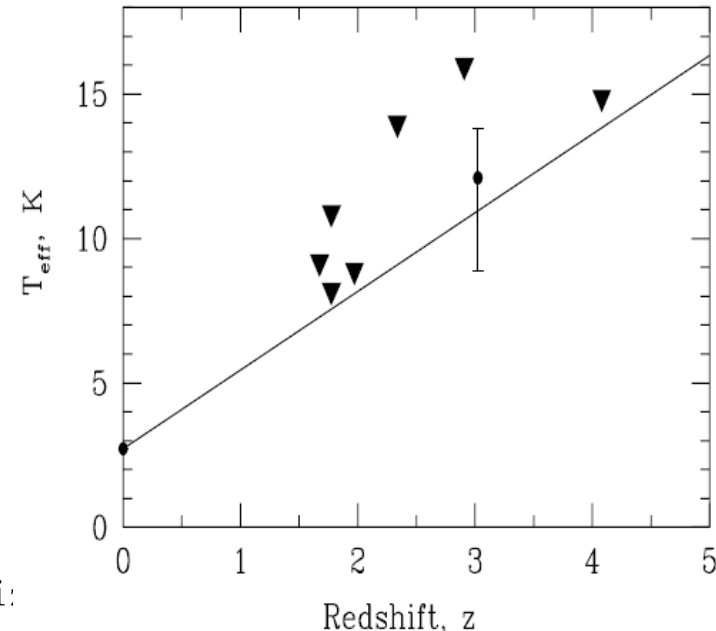


Figure 5 Measurements of the cosmic microwave background radiation temperature at various redshifts. The point at $z = 0$ shows the result of the Cosmic Background Explorer (COBE) determination², $T_{\text{CMBR}}(0) = 2.726 \pm 0.010\text{ K}$. Upper limits are previous measurements^{3,8-10} using the same techniques as we did. We also include our two new unpublished upper limits at $z = 2.1394$ along the line of sight toward Tololo 1037-270. The measurement from this work, $6.0 < T_{\text{CMBR}} < 14.0\text{ K}$ at $z = 2.33771$, is indicated by a vertical bar. The dashed line is the prediction from the hot Big Bang.



Measurement of the T_{CMB} evolution from the Sunyaev-Zel'dovich effect

A & A
2014

G. Hurier¹, N. Aghanim¹, M. Douspis¹, and E. Pointecouteau^{2,3}

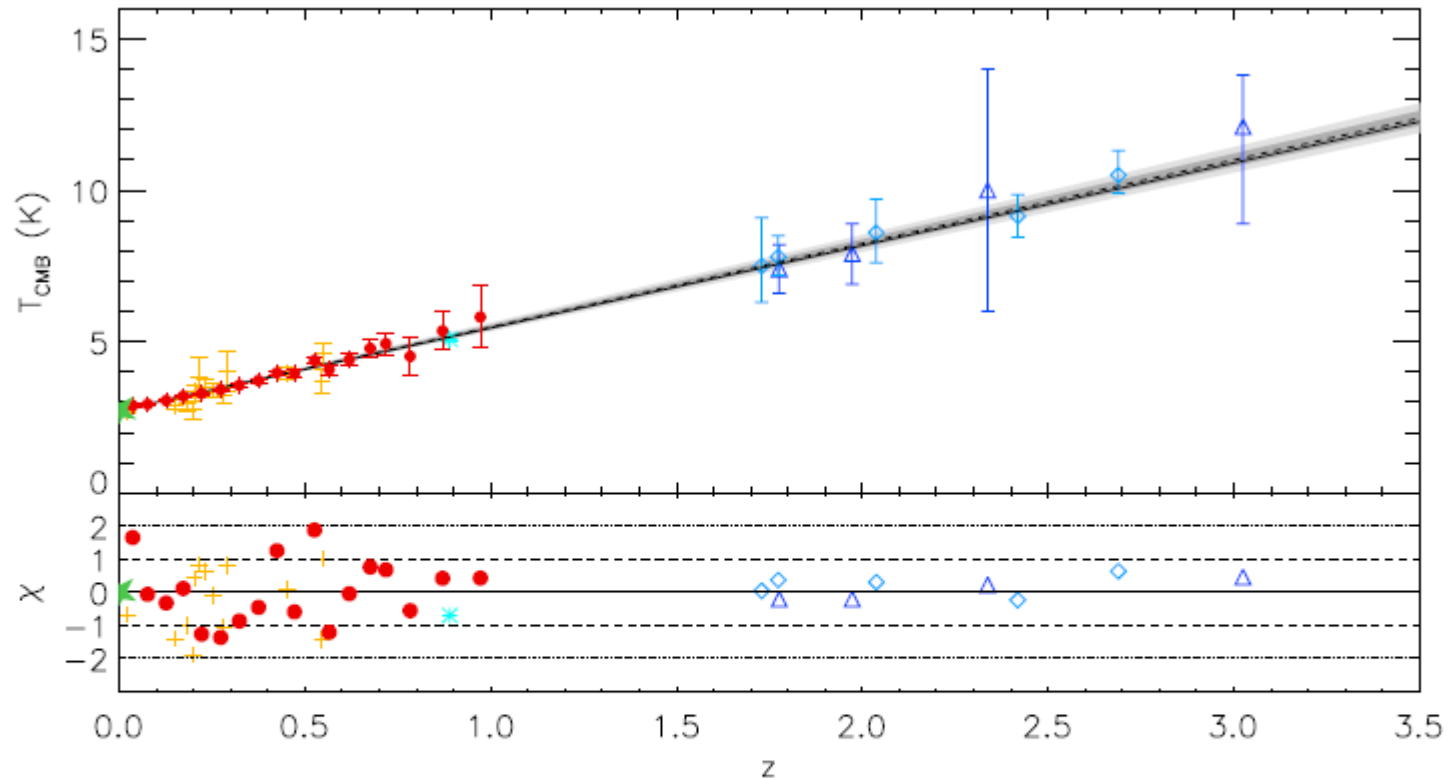


Fig. 8. *Top panel:* T_{CMB} as a function of redshift. The red filled circles represent T_{CMB} measured from the tSZ emission law in redshift bins of *Planck* clusters. The green star shows COBE-FIRAS measurement at $z = 0$ (Fixsen 2009). The orange crosses show T_{CMB} measurements using individual clusters (Battistelli et al. 2002; Luzzi et al. 2009). Dark-blue triangles represent measurements from C_I and C_{II} absorption (Cui et al. 2005; Ge et al. 1997; Srianand et al. 2000; Molaro et al. 2002) at $z = (1.8, 2.0, 2.3, 3.0)$. Blue diamonds show the measurements from CO absorption lines (Srianand et al. 2008; Noterdaeme et al. 2011), and finally the light-blue asterisk is the constraint from various molecular species analyses by Muller et al. (2013). The solid black line presents the standard evolution for T_{CMB} and the dashed black line represents our best-fitting model combining all the measurements. The 1 and 2 σ envelopes are displayed as shaded dark and light-gray regions. *Bottom panel:* deviation from the standard evolution in units of standard deviation. The dashed and dotted black lines correspond to the 1 and 2 σ levels.

Power spectra of curvature and tensor perturbations

$$\mathcal{P}_{\mathcal{R}}(k) = A_s \left(\frac{k}{k_*} \right)^{n_s - 1 + \frac{1}{2} \frac{dn_s}{d \ln k} \ln(k/k_*) + \frac{1}{6} \frac{d^2 n_s}{d \ln k^2} (\ln(k/k_*))^2 + \dots} \quad (10)$$

$$\mathcal{P}_t(k) = A_t \left(\frac{k}{k_*} \right)^{n_t + \frac{1}{2} \frac{dn_t}{d \ln k} \ln(k/k_*) + \dots}, \quad (11)$$

where A_s (A_t) is the scalar (tensor) amplitude and n_s (n_t), $dn_s/d \ln k$ ($dn_t/d \ln k$) and $d^2 n_s/d \ln k^2$ are the scalar (tensor) spectral index, the running of the scalar (tensor) spectral index, and the running of the running of the scalar spectral index, respectively.

Slow-roll scenario as an example

single field, standard kinetic term

The homogeneous evolution of the inflaton field, ϕ , is governed by the equation of motion

$$\ddot{\phi}(t) + 3H(t)\dot{\phi}(t) + V_{\phi} = 0, \quad (1)$$

and the Friedmann equation

$$H^2 = \frac{1}{3M_{\text{pl}}^2} \left(\frac{1}{2}\dot{\phi}^2 + V(\phi) \right). \quad (2)$$

$$r = \frac{\mathcal{P}_t(k_*)}{\mathcal{P}_R(k_*)} \approx 16\epsilon \approx -8n_t, \quad (22)$$

consistency relation. This consistency relation

$$\epsilon_V = \frac{M_{\text{pl}}^2 V_{\phi}^2}{2V^2},$$

$$\eta_V = \frac{M_{\text{pl}}^2 V_{\phi\phi}}{V}.$$

$$A_s \approx \frac{V}{24\pi^2 M_{\text{pl}}^4 \epsilon_V} \quad (13)$$

$$A_t \approx \frac{2V}{3\pi^2 M_{\text{pl}}^4} \quad (14)$$

$$n_s - 1 \approx 2\eta_V - 6\epsilon_V \quad (15)$$

$$n_t \approx -2\epsilon_V \quad (16)$$

$$dn_s/d \ln k \approx -16\epsilon_V \eta_V + 24\epsilon_V^2 + 2\xi_V^2 \quad (17)$$

$$dn_t/d \ln k \approx -4\epsilon_V \eta_V + 8\epsilon_V^2 \quad (18)$$

Constraints on Tensor-to-Scalar Ratio r ($\equiv n_t/n_s$) before 2013.09.

Experiment	Constraint	Goal/Perspective (precision)
WMAP 9	< 0.38	
WMAP 7 + ACT	< 0.28	
WMAP 7 + SPT	< 0.18	
PLANCK + WMAP Polarization	< 0.11 (2σ)	
PLANCK		0.0?
QUIET (1 st session)	$0.35^{+1.06}_{-0.87}$ (43 GHz)	0.1 (43 GHz)
QUIET (2 nd session)	< 2.7 (2σ) (95 GHz)	0.01 (95 GHz)
POLARBEAR		0.007
B-pol, CMB-pol, Litebird		0.001

Gravity waves and non-Gaussian features from particle production in a sector gravitationally coupled to the inflaton

Neil Barnaby,¹ Jordan Moxon,² Ryo Namba,¹ Marco Peloso,¹ Gary Shiu,^{2,3,4} and Peng Zhou²

IV. MODEL II: VECTOR PRODUCED BY A PSEUDOSCALAR INTERACTION

In this section we consider the following model

$$S = \int d^4x \sqrt{-g} \left[\underbrace{\frac{M_p^2}{2} R - \frac{1}{2} (\partial \varphi)^2 - V(\varphi)}_{\text{inflaton sector}} - \underbrace{\frac{1}{2} (\partial \psi)^2 - U(\psi) - \frac{1}{4} F^2 - \frac{\psi}{4f} F \tilde{F}}_{\text{hidden sector}} \right].$$

- ArXiv 1405.0346
- **Blue Tensor Spectrum from particle production during inflation**, Mukohyama, Namba, Peloco, Shiu

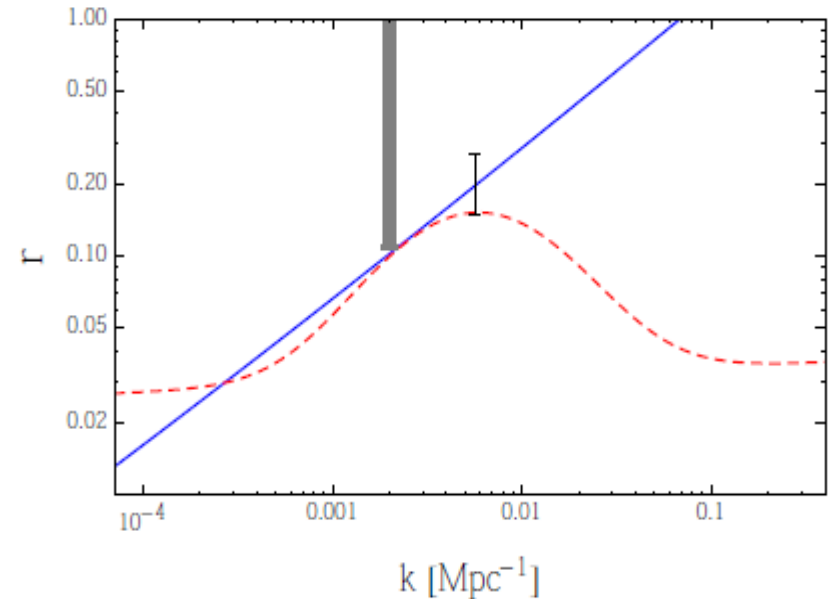
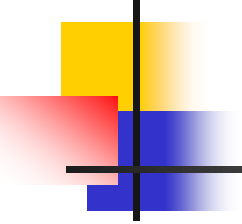


FIG. 4. Two illustrative spectra of the tensor-to-scalar ratio. The blue curve corresponds to the case in Example I, and the red dashed curve to the case in Example II. See the corresponding subsections for the details. The Planck upper bound $r < 0.11$ at $k = 0.002 \text{ Mpc}^{-1}$ and the BICEP2 measurement $r = 0.20^{+0.07}_{-0.05}$ at $k = 0.0057 \text{ Mpc}^{-1}$ ($\ell \approx 80$) are also shown.



Works present in this Workshop relating to Axions and Pseudo scalar-photon (gauge) interactions

- Choi's talk: Implications of the Tensor Mode Detection by BICEP2 for QCD Axion
- Sam Wong's talk: Helical inflation and Cosmic Strings
- Namba's talk tomorrow: Blue Tensor Spectrum from Particle Production during Inflation
- Kodama's talk: Exploring the Axiverse by GWs and γ -rays



Dynamics of Pseudoscalar field

gravitational Lagrangian L_G could be

$$L_G = \left(\frac{1}{16\pi} \right) \times (-g)^{1/2} R(\Gamma^i_{jk}), \quad (28)$$

$$L_G = \left(\frac{1}{16\pi} \right) \times (-g)^{1/2} [R(\Gamma^i_{jk}) + \eta \varphi_{,i} \varphi^{,i}] \quad (29)$$

or

$$L_G = \left(\frac{1}{16\pi} \right) \times (-g)^{1/2} [\varphi R(\{^i_{jk}\}) - (1/\varphi) \omega(\varphi) \varphi_{,i} \varphi^{,i}], \quad (30)$$

where η is a parameter and $\omega(\varphi)$ is a function of φ (Ni 1983c). Various different extensions have been considered, many of them are reviewed in Balakin and Ni (2010).

Exploring the Axiverse and Bosenova 'stars' by CPR

- Monday talk by **Kodama-san**: Exploring the Axiverse by **GWs** and **γ -rays**

A 4-point **P1** on
Last Scattering
Surface

Bosenova
'stars'

Dectector
At 4-point **P2**

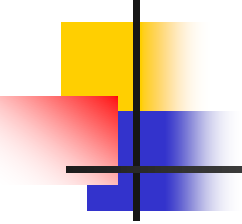
- CPR rotation in phase: $\xi[\varphi(P2) - \varphi(P1)]$ classically, independent of the Bosenova pseudoscalar potential if it does not influence the P1 potential**
- Quantum effects may need to and can be studied through absorption, i.e., dichroism (due to pol-dependent absorption)**

Three approaches to Axions/Pseudoscalar-photon interactions

- Top down approach – string theory
- Bottom up approach – QCD axion
- Phenomenological approach -- gravitation

Table 1. Various terms in the Lagrangian and their meaning.

Term	Dimension	Reference	Meaning
$e^{\alpha\beta\gamma} A_\alpha F_{\beta\gamma}$	3	Chern–Simons (1974)	Intergrand for topological invariant
$e^{ijkl} \varphi F_{ij} F_{kl}$	4	Ni (1973, 1974, 1977)	Pseudoscalar-photon coupling
$e^{ijkl} \varphi F_{ij}^{\text{QCD}} F_{kl}^{\text{QCD}}$	4	Peccei–Quinn (1977) Weinberg (1978) Wilczek (1978)	Pseudoscalar-gluon coupling
$e^{ijkl} V_i A_j F_{kl}$	4	Carroll–Field–Jackiw (1990)	External constant vector coupling



φ : Pseudoscalar field or
pseudoscalar function of
gravitational or relevant fields

$$\mathcal{L}_{\text{int}} \sim \rho_{\mu} A_{\nu} \tilde{F}^{\mu\nu},$$

$$\begin{aligned} &\approx \xi \varphi_{,\mu} A_{\nu} F^{\sim\mu\nu} \\ &\approx \xi (1/2) \varphi F_{\mu\nu} F^{\sim\mu\nu} \end{aligned}$$

(Mod Divergence)

Einstein Equivalence Principle

EEP

- Minimal coupling \leftrightarrow EEP
- We heard of **nonminimal couplings** in **this workshop**
- Looking for **theoretical and empirical foundations of EEP** is important
- I started in 1972 to work on this

Galileo EP → Electromagnetism: Charged particles and photons

Special Relativity

$$L_I = -\left(\frac{1}{16\pi}\right)\eta^{ijkl}\eta^{jl}F_{ij}F_{kl} - A_k j^k (-g)^{1/2} - \sum_I m_I \frac{ds_I}{dt} \delta(x - x_I)$$

χ – gframework

$$L_I = -\left(\frac{1}{16\pi}\right)\chi^{ijkl}F_{ij}F_{kl} - A_k j^k (-g)^{1/2} - \sum_I m_I \frac{ds_I}{dt} \delta(x - x_I)$$

Galileo EP constrains χ :

$$\chi^{ijkl} = (-g)^{1/2} \left[\frac{1}{2} g^{ik} g^{jl} - \frac{1}{2} g^{il} g^{kj} + \eta \phi \varepsilon^{ijkl} \right]$$

(Pseudo)scalar-Photon
Interaction



Pseudo-scalars: Pseudoscalar-Photon Coupling

PHYSICAL REVIEW LETTERS

VOLUME 38

14 FEBRUARY 1977

NUMBER 7

Equivalence Principles and Electromagnetism*

Wei-Tou Ni

Department of Physics, Montana State University, Bozeman, Montana 59715, and Department of Physics, National Tsing Hua University, Hsinchu, Taiwan, Republic of China†

(Received 16 June 1976)

The implications of the weak equivalence principles are investigated in detail for electromagnetic systems in a general framework. In particular, I show that the universality of free-fall trajectories {Galileo weak equivalence principle (WEP[I])} does not imply the validity of the Einstein equivalence principle (EEP). However, WEP[I] plus the universality of free-fall rotation states (WEP[II]) does imply EEP. To test WEP[II] and EEP, I suggest that Eötvös-type experiments on polarized bodies be performed.

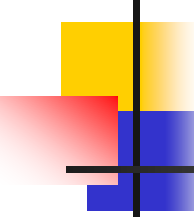
$$\mathcal{L}_I = - \left(\frac{1}{16\pi} \right) \chi^{ijkl} F_{ij} F_{kl} - A_k j^k (-g)^{1/2} - \sum_I m_I \frac{ds_I}{dt} \delta(\vec{x} - \vec{x}_I),$$

Theorem I.—For a system whose Lagrangian density is given by (1), WEP[I] holds if and only if

$$\chi^{ijkl} = (-g)^{1/2} \left(\frac{1}{2} g^{ik} g^{jl} - \frac{1}{2} g^{il} g^{kj} + \varphi \epsilon^{ijkl} \right), \quad (9)$$

where φ is a scalar function of the gravitational fields and $\epsilon^{ijkl} = (-g)^{1/2} e^{ijkl}$.—In a Fermi-normal

The nonmetric theory given by Eq. (9) may be related to the existence of parity-nonconserving field or spontaneously broken symmetry. Since these concepts are quite fruitful in weak interactions and in obtaining unified weak and electromagnetic theories, serious efforts deserve to be spent in this direction for gravitation. Detailed analyses of this nonmetric theory and the Eötvös-type experiments on polarized bodies will be presented elsewhere.



For the gravity theory (21) with an effective pseudoscalar, discussed in sections 2.4 and 3.4, the electromagnetic wave propagation equation is given by equation (23). In a local inertial (Lorentz) frame of the g -metric, it is reduced to

$$F^{ik}{}_{,k} + e^{ikml} F_{km} \varphi_{,l} = 0. \quad (51)$$

Analyzing the wave into Fourier components, imposing the radiation gauge condition and solving the dispersion eigenvalue problem, we obtain $k = \omega + (n^\mu \varphi_{,\mu} + \varphi_{,0})$ for right circularly polarized wave and $k = \omega - (n^\mu \varphi_{,\mu} + \varphi_{,0})$ for left circularly polarized wave in the eikonal approximation (Ni 1973, Carroll *et al* 1990). Here n^μ is the unit 3-vector in the propagation direction. The group velocity is

$$v_g = \partial\omega/\partial k = 1, \quad (52)$$

independent of polarization. There is no birefringence.



The ISSUE of testing EEP is the issue of deriving the spacetime structure from experiments

- First step: How to derive spacetime structure/the light cone from classical, local and linear electrodynamics
- EEP for light: (i) trajectory independent of frequency (photon energy) and polarization: no birefringence
(ii) no polarization rotation (w.r.t matter spin)



Framework for testing EEP

Maxwell equations in terms of field strength $F_{kl}(\mathbf{E}, \mathbf{B})$ and excitation $H^{ij}(\mathbf{D}, \mathbf{H})$ do not need metric as primitive concept. Field strength $F_{kl}(\mathbf{E}, \mathbf{B})$ and excitation $H^{ij}(\mathbf{D}, \mathbf{H})$ can all be independently defined operationally [1]. To complete this set of equations, one needs the constitutive relation between the excitation and the field in both macroscopic electrodynamics and in space-time theory of gravity:

$$H^{ij} = (1/2) \chi^{ijkl} F_{kl}. \quad (1)$$

When Einstein Equivalence Principle is observed, this fundamental space-time tensor density is induced by the metric g^{ij} of the form

$$\chi^{ijkl} = (1/2) (-g)^{1/2} (g^{ik} g^{jl} - g^{il} g^{kj}), \quad (g \equiv (\det g^{ij})^{-(1/2)}) \quad (2)$$

and the Maxwell equations can be derived from a Lagrangian density. In local inertial



Constitutive Law

- To complete this set of Maxwell equations, one needs a **constitutive relation** between the excitation and the field:

$$H^{ij} = (1/2) \chi^{ijkl} F_{kl}.$$

- Since both H^{ij} and F_{kl} are antisymmetric, χ^{ijkl} must be antisymmetric in i and j , and k and l . Hence χ^{ijkl} has 36 independent components.



Decomposition of the constitutive tensor

$$\chi^{ijkl} = {}^{(P)}\chi^{ijkl} + {}^{(Sk)}\chi^{ijkl} + {}^{(A)}\chi^{ijkl}, \quad (\chi^{ijkl} = -\chi^{jikl} = -\chi^{ijlk})$$

$${}^{(P)}\chi^{ijkl} = (1/6)[2(\chi^{ijkl} + \chi^{klij}) - (\chi^{iklj} + \chi^{ljik}) - (\chi^{iljk} + \chi^{jkil})],$$

$${}^{(A)}\chi^{ijkl} = \chi^{[ijkl]} = \varphi e^{ijkl},$$

$${}^{(Sk)}\chi^{ijkl} = (1/2)(\chi^{ijkl} - \chi^{klij}),$$

- Principal part: 20 degrees of freedom
- Axion part: 1 degree of freedom
(Ni 1973,1974,1977; Hehl et al. 2008 Cr2O3)
- Skewon part: 15 degrees of freedom
(Hehl-Ohbukhov-Rubilar skewon 2002)

Skewonless EM wave propagation in local linear electrodynamics

Since our galactic Newtonian potential U is of the order of 10^{-6} , we use weak field approximation in the χ -g framework. The vacuum Maxwell equation, derived from the Lagrangian (9), is

$$(\chi^{ijkl} A_{k,\ell})_{,j} = 0. \quad (19)$$

Neglecting $\chi^{ijkl}_{,p}$ in slowly varying field, (19) becomes

$$\chi^{ijkl} A_{k,\ell j} = 0. \quad (20)$$

For weak field, we assume

$$\chi^{ijkl} = \chi^{(0)ijkl} + \chi^{(1)ijkl}, \quad (21)$$

where

$$\chi^{(0)ijkl} = \frac{1}{2} \eta^{ik} \eta^{jl} - \frac{1}{2} \eta^{il} \eta^{kj} \quad (22)$$

with η^{ij} the Minkowski metric and $|\chi^{(1)ij}| \ll 1$.

Dispersion relation and Nonbirefringence condition

B. Conditions for gravitational nonbirefringence — Photons propagate along a metric H_{ik}

Using eikonal approximation, we look for plane-wave solution propagating in the z -direction. Imposing radiation condition in the zeroth order and solving the dispersion relation for ω , we obtain

$$\omega_{\pm} = k \left\{ 1 + \frac{1}{4} \left[(K_1 + K_2) \pm \sqrt{(K_1 - K_2)^2 + 4K^2} \right] \right\} \quad (23)$$

where

$$\begin{aligned} K_1 &= \chi^{(1)1010} - 2\chi^{(1)1013} + \chi^{(1)1313}, \\ K_2 &= \chi^{(1)2020} - 2\chi^{(1)2023} + \chi^{(1)2323}, \\ K &= \chi^{(1)1020} - \chi^{(1)1023} - \chi^{(1)1320} + \chi^{(1)1323}. \end{aligned} \quad (24)$$

Photons with two different polarizations propagate with different speed $v_{\pm} = \frac{\omega_{\pm}}{k}$ and would split in 4-dimensional spacetime. The conditions for no splitting (no retardation) is $\omega_{+} = \omega_{-}$, i.e.

$$K_1 = K_2, \quad K = 0. \quad (25)$$

(25) gives two constraints on $\chi^{(1)}$'s.

The conditions for no splitting (no retardation) of electromagnetic waves propagating in every direction give the following ten constraints on $\chi^{(1)}$'s:

$$\begin{aligned}
 \chi^{(1)1010} + \chi^{(1)1313} &= \chi^{(1)2020} + \chi^{(1)2323} , \\
 \chi^{(1)1220} &= \chi^{(1)1330} , & \chi^{(1)1010} + \chi^{(1)1212} &= \chi^{(1)3030} + \chi^{(1)3232} . \\
 \chi^{(1)2330} &= \chi^{(1)2110} , & \text{ne } H^{(1)ij} , \psi \text{ and } \phi \text{ as} \\
 \chi^{(1)3110} &= \chi^{(1)3220} , & H^{(1)10} \equiv H^{(1)01} &\equiv -2\chi^{(1)1220} , \\
 \chi^{(1)1020} &= -\chi^{(1)1323} , & H^{(1)20} \equiv H^{(1)02} &\equiv -2\chi^{(1)2330} , \\
 \chi^{(1)2030} &= -\chi^{(1)2131} , & H^{(1)30} \equiv H^{(1)03} &\equiv -2\chi^{(1)3110} , \\
 \chi^{(1)3010} &= -\chi^{(1)3212} , & H^{(1)12} \equiv H^{(1)21} &\equiv -2\chi^{(1)1020} , \\
 \chi^{(1)1320} &= -\chi^{(1)1230} , & H^{(1)23} \equiv H^{(1)32} &\equiv -2\chi^{(1)2030} , \\
 \chi^{(1)1320} &= -\chi^{(1)2310} , & H^{(1)31} \equiv H^{(1)13} &\equiv -2\chi^{(1)3010} , \\
 & & H^{(1)11} &\equiv 2\chi^{(1)2020} + 2\chi^{(1)2121} - H^{(1)00} , \\
 & & H^{(1)22} &\equiv 2\chi^{(1)3030} + 2\chi^{(1)3232} - H^{(1)00} , \\
 & & H^{(1)33} &\equiv 2\chi^{(1)1010} + 2\chi^{(1)1313} - H^{(1)00} , \\
 & & \psi &\equiv 1 + 2\chi^{(1)1212} + \frac{1}{2}\eta_{00}(H^{(1)00} - H^{(1)11} - H^{(1)22} \\
 & & &\quad - H^{(1)33}) - H^{(1)11} - H^{(1)22} , \\
 & & \phi &\equiv \chi^{(1)0123} .
 \end{aligned}$$

Note that in these definitions $H^{(1)00}$ is not defined and free. It is straightforward to show that if the ten constraints (26) are satisfied then χ can be written to first-order in $\chi^{(1)}$'s in the form

$$\chi^{ijkl} = (-H)^{\frac{1}{2}} \left(\frac{1}{2} H^{ik} H^{jl} - \frac{1}{2} H^{il} H^{kj} \right) \psi + \phi e^{ijkl}, \quad (28)$$

where

$$H^{ij} = \eta^{ij} + H^{(1)ij},$$

$$H = \det(H_{ij}), \quad (29)$$

$$H_{ij} H^{jk} = \delta_i^k,$$

and

$$e^{ijkl} = \begin{cases} 1, & \text{if } (ijkl) \text{ is an even permutation of } (0123), \\ -1, & \text{if } (ijkl) \text{ is an odd permutation of } (0123), \\ 0, & \text{otherwise.} \end{cases} \quad (30)$$

Table II. Empirical Foundations of the Einstein Equivalence Principle.

Experiments	Constraints	Accuracy
Pulsar Signal Propagation	$\chi^{ijkl} \rightarrow (-H)^{\frac{1}{2}} \left(\frac{1}{2} H^{ik} H^{jl} - \frac{1}{2} H^{il} H^{kj} \right) \psi + \phi e^{ijkl}$	$10^{-8} - 10^{-10}$
Hughes-Drever Experiments	$H_{\mu\nu} \rightarrow g_{\mu\nu}$	10^{-12}
	$H_{0\mu} \rightarrow g_{0\mu}$	$10^{-7} - 10^{-8}$
	$H_{00} \rightarrow g_{00}$	10^{-4}
Eötvös-Dicke-Braginsky Experiments	$\psi \rightarrow 1$	10^{-9}
	$H_{00} \rightarrow g_{00}$	10^{-5}
Vessot-Levine Redshift Experiment	$H_{00} \rightarrow g_{00}$	10^{-4}

* With the above constraints, $\chi^{ijkl} = (-g)^{\frac{1}{2}} \left(\frac{1}{2} g^{ik} g^{jl} - \frac{1}{2} g^{il} g^{kj} \right) + \phi e^{ijkl}$ to various degrees of accuracy, i.e. EEP is verified to various degrees of accuracy except for the freedom in ϕ .

Observational Constraints from Pulsars

C. Observational constraints from pulsars.

In actual observations, the pulses and micropulses with different polarizations are correlated in general structure and no retardation with respect to polarizations are observed. This means that conditions similar to (25) are satisfied to observational accuracy. For Crab pulsar, the micropulses with different polarizations are correlated in timing to within 10^{-4} sec, the distance of the Crab pulsar is 2200 pc, therefore to within 10^{-4} sec / (2200 x 3.26 light yr.) = 5×10^{-16} accuracy two conditions similar to (25) are satisfied. Over 300 pulsars in different directions are observed. Many of them have polarization data. Combining all of them, (26) is satisfied to an accuracy of 10^{-14} - 10^{-16} . Since $U \sim 10^{-6}$, $\chi^{(1)}/U$ (or χ/U) agrees with that given by (28) to an accuracy of 10^{-8} - 10^{-10} . Detailed analysis will reveal better results.

Thus, to high accuracy, photons are propagating in the metric field H^{ik} and two additional scalar fields ϕ and ψ . A change of H^{ik} to λH^{ik} does not affect χ^{ijkl} in (28) — this corresponds to the freedom of $H^{(1)00}$ in the definition (27) of $H^{(1)ij}$. Thus we have eleven degrees of freedom in (28).

Outlook for the future at 1983

extra-galactic pulsars & optical/X-ray observations

Recently, McCulloch, Hamilton, Ables and Hunt⁴² have observed a radio pulsar in the large Magellanic Cloud. Backer, Kulkarni, Heiles, Davis and Goss⁴³ have discovered a millisecond pulsar which rotates 20 times faster than the Crab pulsar. The progress of these observations would potentially give better constraints on some of the conditions (26) due to larger distance or fast period involved.

Analysis of optical and X-ray polarization data from various astrophysical sources will give better accuracy to some of the ten constraints in (26). Results of this analysis will be presented in the future.

■ Now constraining to 10^{-32}

Amplification/dissipation constraint

In this section we look into the observations/experiments to constrain the skewon field contribution to spacetime constitutive tensor density. If ξ as defined in (36) is less than zero, i.e. $(A_{(1)} - A_{(2)})^2 + 4({}^{(P)}B)^2 < 4({}^{(Sk)}B)^2$, the dispersion relation (34) is

$$\omega = k [1 + \frac{1}{2} (A_{(1)} + A_{(2)}) \pm \frac{1}{2} (-\xi)^{1/2} i] + O(2). \quad \text{Redshift } kt \rightarrow \quad (50)$$

The exponential factor in the wave solution (23) is of the form

$$\int k(t) dt = \int k(t_0)(1 + z(t)) dt \equiv (1 + \langle z(t) \rangle) k(t_0)(t_0 - t_1).$$

$$\exp(ikz - i\omega t) \sim \exp[ikz - ik(1 + \frac{1}{2}(A_{(1)} + A_{(2)}))t] \exp(\pm \frac{1}{2}(-\xi)^{1/2}kt). \quad (51)$$

There are both dissipative and amplifying wave propagation modes. In the small ξ limit, the amplification/attenuation factor $\exp(\pm \frac{1}{2}(-\xi)^{1/2}kt)$ equals $[1 \pm \frac{1}{2}(-\xi)^{1/2}kt]$ to a very good approximation. Since this factor depends on the wave number/frequency, it will distort the source spectrum in propagation.

Type I skewons are constrained to $|^{(\text{SkI})}\chi^{ijkl}|$ to \leq a few $\times 10^{-35}$

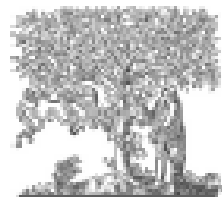
For the highest frequency band ω is $2\pi \times 857$ GHz. The amplification/dissipation in fraction is

$$\frac{1}{2}(-\xi)^{1/2}k \times 45.328 \text{ Gyr} = 3.8 \times 10^{30} (-\xi)^{1/2}. \quad (53)$$

For the lowest frequency band ω is $2\pi \times 30$ GHz; the effect is about $\pm 3.5\%$ of (53). From CMB observations that the spectrum is less than 10^{-4} deviation, we have

$$(-\xi)^{1/2} < 2.6 \times 10^{-35}. \quad (54)$$

$$\frac{1}{2}(-\xi)^{1/2} = |^{(\text{Sk})}B| = \frac{1}{2}|(B_{(1)} - B_{(2)})| = |^{(\text{Sk})}\chi^{(1)1020} + ^{(\text{Sk})}\chi^{(1)1323} - ^{(\text{Sk})}\chi^{(1)1023} - ^{(\text{Sk})}\chi^{(1)1320}| < 1.3 \times 10^{-35}, \quad (55)$$



ELSEVIER

Contents lists available at ScienceDirect

Physics Letters A

www.elsevier.com/locate/pla



Skewon field and cosmic wave propagation

Wei-Tou Ni

Center for Gravitation and Cosmology, Department of Physics, National Tsing Hua University, Hsinchu, 30013, Taiwan, ROC

ARTICLE INFO

Article history:

Received 11 December 2013

Received in revised form 26 February 2014

Accepted 28 February 2014

Available online xxxxx

Communicated by P.R. Holland

Keywords:

Classical electrodynamics

Skewon field

General relativity

Equivalence principle

Dilaton field

Axion field

ABSTRACT

We study the propagation of the Hehl–Obukhov–Rubilar skewon field in weak gravity field/dilute matter or with weak violation of the Einstein Equivalence Principle (EEP), and further classify it into Type I and Type II skewons. From the dispersion relation we show that no dissipation/no amplification condition implies that the additional skewon field must be of Type II. For Type I skewon field, the dissipation/amplification is proportional to the frequency and the CMB spectrum would deviate from Planck spectrum. From the high precision agreement of the CMB spectrum with 2.755 K Planck spectrum, we constrain the Type I cosmic skewon field $|(^{SK0})\chi^{ijkl}|$ to \leq a few $\times 10^{-35}$. The skewon part of constitutive tensor constructed from asymmetric metric is of Type II, hence it is allowed. This study may also help application in macroscopic electrodynamics in the case of laser pumped medium or dissipative medium.

© 2014 Published by Elsevier B.V.

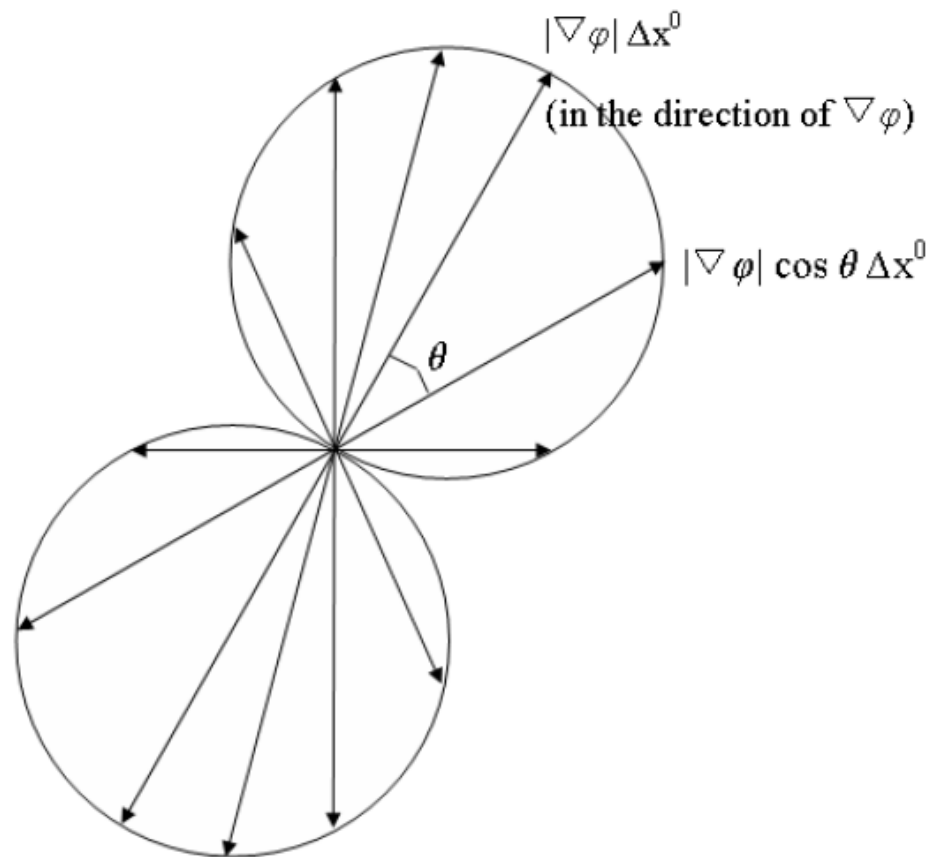
Cosmic Polarization Rotation:

- (i) test fundamental law of EM propagation;
- (ii) map the cosmic pseudoscalar field

For the right circularly polarized electromagnetic wave, the propagation from a point $P_1 = \{x_{(1)}^i\} = \{x_{(1)}^0; x_{(1)}^\mu\} = \{x_{(1)}^0, x_{(1)}^1, x_{(1)}^2, x_{(1)}^3\}$ to another point $P_2 = \{x_{(2)}^i\} = \{x_{(2)}^0; x_{(2)}^\mu\} = \{x_{(2)}^0, x_{(2)}^1, x_{(2)}^2, x_{(2)}^3\}$ adds a phase of $\alpha = \varphi(P_2) - \varphi(P_1)$ to the wave; for left circularly polarized light, the added phase will be opposite in sign (Ni 1973). Linearly polarized electromagnetic wave is a superposition of circularly polarized waves. Its polarization vector will then rotate by an angle α . Locally, the polarization rotation angle can be approximated by

$$\begin{aligned}\alpha &= \varphi(P_2) - \varphi(P_1) = {}_i \Sigma_0^3 [\varphi_{,i} \times (x_{(2)}^i - x_{(1)}^i)] \\ &= {}_i \Sigma_0^3 [\varphi_{,i} \Delta x^i] = \varphi_{,0} \Delta x^0 + [{}_\mu \Sigma_1^3 \varphi_{,\mu} \Delta x^\mu] \\ &= {}_i \Sigma_0^3 [V_i \Delta x^i] = V_0 \Delta x^0 + [{}_\mu \Sigma_1^3 V_\mu \Delta x^\mu].\end{aligned}\tag{53}$$

Space contribution to the local polarization rotation angle -- $[\mu\Sigma_{13}\varphi, \mu\Delta x\mu] = |\nabla\varphi| \cos\theta \Delta x^0$. The time contribution is $\varphi, \theta \Delta x^0$. The total contribution is $(|\nabla\varphi| \cos\theta + \varphi, \theta) \Delta x^0$. ($\Delta x^0 > 0$)



Integrated:

$\varphi(2) - \varphi(1)$

1: a point at the decoupling epoch

2: observation point



Variations and Fluctuations

- *Rotation $\varphi(2) - \varphi(1)$*
- *$\delta\varphi(2) - \delta\varphi(1)$: $\delta\varphi(2)$ variations and fluctuations at the last scattering surface of the decoupling epoch; $\delta\varphi(1)$, at present observation point, fixed*
- *$\langle [\delta\varphi(2) - \delta\varphi(1)]^2 \rangle$ variance of fluctuation $\sim [\text{coupling} \xi \times 10^{(-5)}]^2$*
- *The coupling depends on various cosmological models*

Exploring the Axiverse and Bosenova 'stars' by CPR

- Monday talk by **Kodama-san**: Exploring the Axiverse by **GWs** and **γ -rays**

A 4-point **P1** on
Last Scattering
Surface

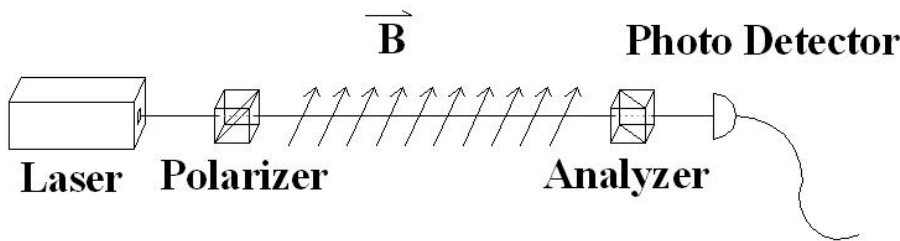
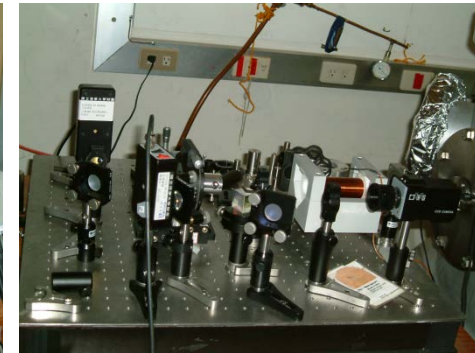
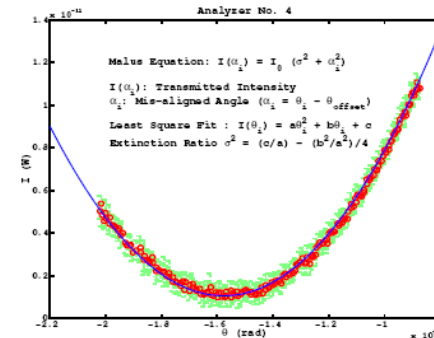
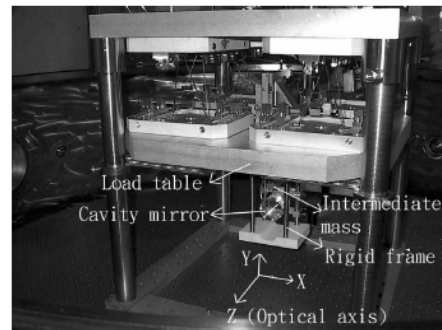
Bosenova
'stars'

Dectector
At 4-point **P2**

- CPR rotation in phase: $\xi[\varphi(P2) - \varphi(P1)]$ classically, independent of the Bosenova pseudoscalar potential if it does not influence the P1 potential**
- Quantum effects may need to and can be studied through absorption, i.e., dichroism (due to pol-dependent absorption)**

Q & A Experiment and Measuring the parameters of the PPM electrodynamics

$$\Delta n = n_{\parallel} - n_{\perp} = 4.0 \times 10^{-24} (\mathbf{B}^{\text{ext}}/1\text{T})^2$$



Vacuum Dichroism, Pseudoscalar-Photon Interaction and Millicharged Fermions 2821

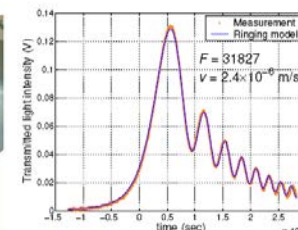
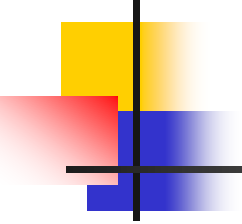


Fig. 3. A picture of experimental apparatus.

Fig. 4. A finesse measurement with fitting.

Constraints on cosmic polarization rotation from CMB



Reference	Constraint [mrad]	Source data
Ni(2005) ^{5,6}	± 100	WMAP1(2003) ¹
Feng, Li, Xia, Chen, and Zhang(2006) ⁷	-105 ± 70	WMAP3 ² & BOOMERANG (B03) ³
Liu, Lee, Ng(2006) ⁸	± 24	BOOMERANG (B03) ³
Kostelecky and Mews(2007) ⁹	209 ± 122	BOOMERANG (B03) ³
Cabella, Natoli and Silk(2007) ¹⁰	-43 ± 52	WMAP3 ⁴
Xia, Li, Wang, and Zhang(2007) ¹¹	-108 ± 67	WMAP3 ² & BOOMERANG (B03) ³
Komatsu, et al.(2008) ¹²	-30 ± 37	WMAP5 ⁴
Xia, Li, Zhao, and Zhang(2008) ¹³	-45 ± 33	WMAP5 ⁴ & BOOMERANG (B03) ³



WMAP9 and BICEP1 Constraints

Experiment	Frequency	Multipoles	CPR angle	Reference
WMAP9	41,61,94 GHz	2-800	$-0.36^\circ \pm 1.24^\circ \pm 1.5^\circ$	Hinshaw et al 2012
BICEP1	100,150 GHz	20-335	$-2.77^\circ \pm 0.86^\circ \pm 1.3^\circ$	Kaufman et al 2014

The rotation angle given by the revision of BICEP1 data by Kaufman et al. (2014) formally corresponds to a 1.78 sigma detection of CPR. However, taking into account the uncertainties involved in the calibration of the BICEP1 polarization angle, the problems in correcting for galactic Faraday rotation, (Section VI.B of Kaufman et al. 2014), and the inconsistency of this result with the one of QUaD, for which Brown et al. (2009) give a CPR angle of $0.64^\circ \pm 0.5^\circ(\text{stat.}) \pm 0.5^\circ(\text{syst.})$, we do not consider this CPR “detection” as final. Recently Gubitosi and Paci (2013) have reviewed the constraints on CPR, but they have considered only those deriving from CMB polarization data.

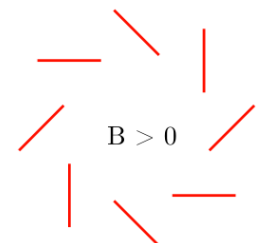
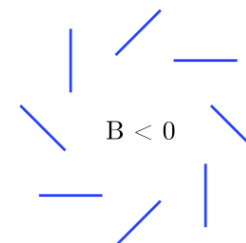
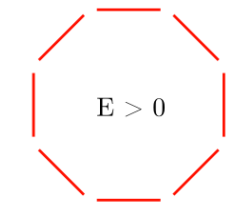
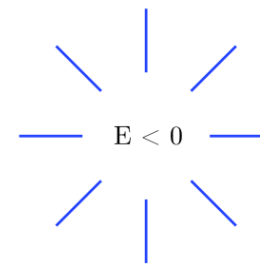
Constraints on Cosmic Polarization

Rotation $\phi(x, y, z, t; x_0, y_0, z_0, t_0)$

Method	CB rotation	Distance	Direction	Ref.
RG radio pol.	$ \theta < 6^\circ$	$0.4 < z < 1.5$	all-sky (uniformity ass.)	
RG radio pol.	$\theta = -0.6^\circ \pm 1.5^\circ$	$\langle z \rangle = 0.78$	all-sky (uniformity ass.)	
RG UV pol.	$\theta = -1.4^\circ \pm 1.1^\circ$	$z = 0.811$	<i>RA: 176.37°, Dec: 31.56°</i>	
RG UV pol.	$\theta = -0.8^\circ \pm 2.2^\circ$	$\langle z \rangle = 2.80$	all-sky (uniformity ass.)	
RG UV pol.	$\langle \theta^2 \rangle \leq (3.7^\circ)^2$	$\langle z \rangle = 2.80$	all-sky (stoch. var.)	
CMB pol. BOOMERanG	$\theta = -4.3^\circ \pm 4.1^\circ$	$z \sim 1100$	all-sky (uniformity ass.)	
CMB pol. QUAD	$\theta = 0.64^\circ \pm 0.71^\circ$	$z \sim 1100$	all-sky (uniformity ass.)	
CMB pol. BICEP	$\theta = -2.6^\circ \pm 1.2^\circ$	$z \sim 1100$	all-sky (uniformity ass.)	
CMB pol. WMAP7	$\theta = -1.1^\circ \pm 2.0^\circ$	$z \sim 1100$	all-sky (uniformity ass.)	

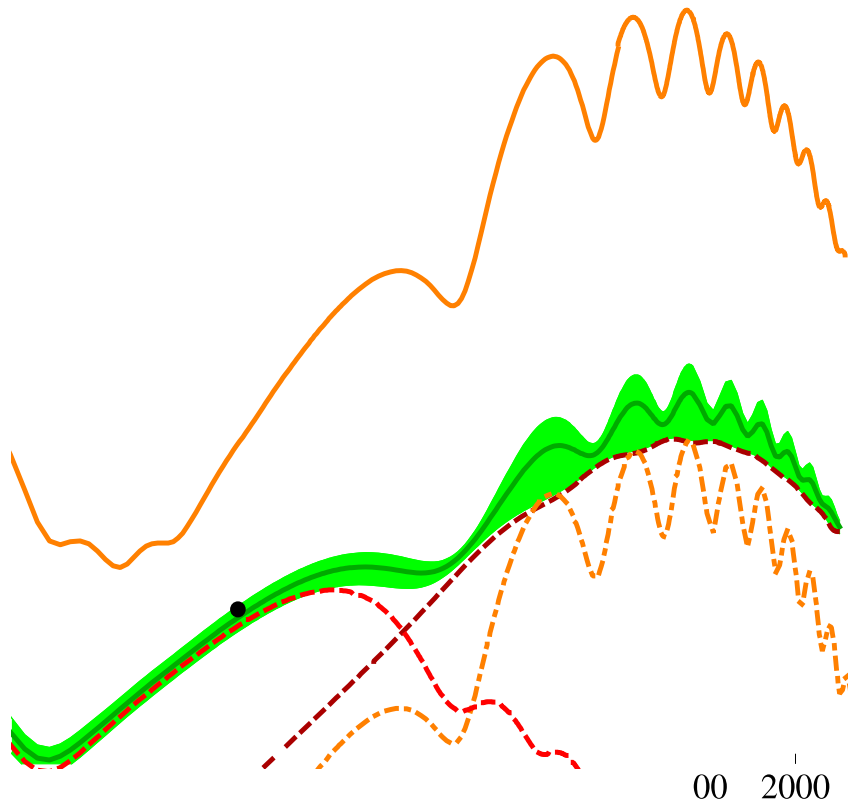
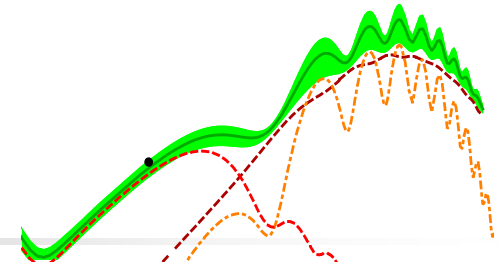
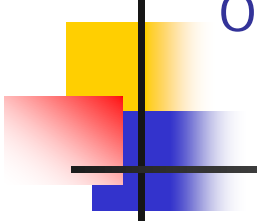
Three processes can produce CMB B-mode polarization observed

- (i) gravitational lensing from E-mode polarization (Zaldarriaga & Seljak 1997),
- (ii) local quadrupole anisotropies in the CMB within the last scattering region by large scale GWs (Polnarev 1985)
- (iii) cosmic polarization rotation (CPR) due to pseudoscalar-photon interaction (Ni 1973; for a review, see Ni 2010).
(The CPR has also been called **Cosmological Birefringence**)



NEW CONSTRAINTS ON COSMIC POLARIZATION ROTATION FROM DETECTIONS OF B-MODE POLARIZATION IN CMB

Alighieri, Ni and Pan



Tensor B ($r = 0.188$)

For CPR fluctuation in a patch of sky, the rotated B-mode ℓ -power spectrum $C_l^{BB,obs}$ from E-mode power C_l^{EE} for $\ell > 30$ and for small CPR angle $\underline{\alpha}$ is accurately given by

$$C_l^{BB,obs} \approx C_l^{EE} \sin^2(2\underline{\alpha}) \approx 4\underline{\alpha}^2 C_l^{EE}. \quad (12)$$

This can be shown by comparing the E-mode power spectrum from Figure 10 of Lewis & Challinor (2006) and the B-mode power spectrum from Fig. 5 of Zhao & Li. They are almost identical up to a scale $4\underline{\alpha}^2$.

The present BICEP2 data group about 20 azimuthal eigen-modes into one band; $\zeta(\ell)$ is virtually equal to one. We will set it to ℓ in our analysis. For precise measurement of variations/fluctuations, direct processing of data without first evaluation of the ℓ components may be an alternative method.

- BICEP2 had made about 1 degree global (whole patch) de-rotation for B-mode

In the propagation, E-mode polarization will rotate into B-mode polarization with $\sin^2 2\alpha$ ($\approx 4\alpha^2$ for small α) fraction of power. For uniform rotation across the sky, the azimuthal eigenvalue ℓ is invariant under polarization rotation and does not change. For small angle,

$$\alpha = \varphi(\mathbf{P}_2) - \varphi(\mathbf{P}_1) = [\varphi(\mathbf{P}_2) - \varphi(\mathbf{P}_1)]_{\text{mean}} + \delta\varphi(\mathbf{P}_1), \quad (9)$$

$$\underline{\alpha}^2 \equiv \langle \alpha^2 \rangle = ([\varphi(\mathbf{P}_2) - \varphi(\mathbf{P}_1)]_{\text{mean}})^2 + \delta\varphi^2(\mathbf{P}_1), \quad (10)$$

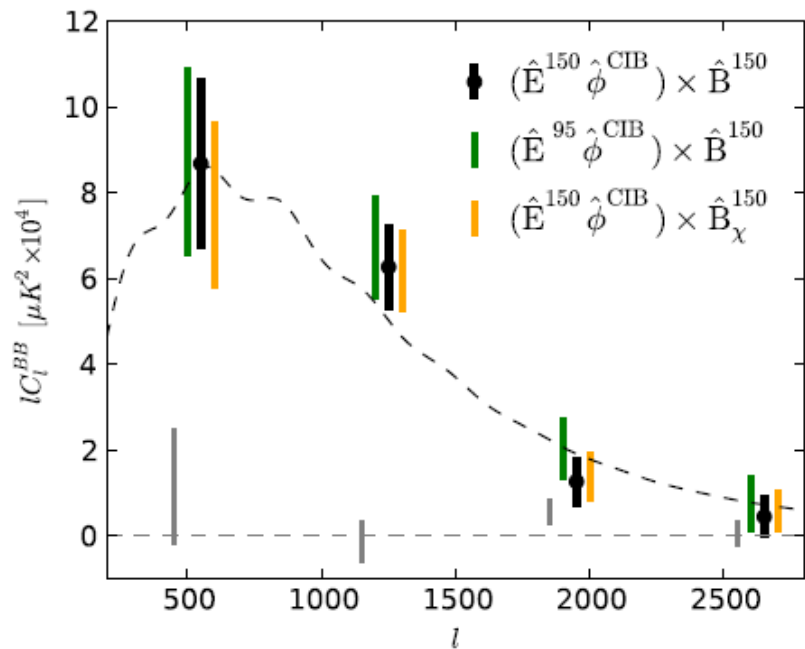
where $\underline{\alpha} \equiv \langle \alpha^2 \rangle^{1/2}$ is the root mean-square-sum polarization rotation angle.

In translating the power distribution to azimuthal eigenvalue variable ℓ , we need to insert a factor $\zeta(\ell) \approx \ell$ in front of $\delta_1 \varphi^2(2)$ to take care of the nonlinear conversion to ℓ due to fluctuations. For uniform rotation with angle α across the sky, the rotation of (original) E-mode power C_l^{EE} into B-mode power $C_l^{BB, \text{obs}}$ is given by (see, e.g., Zhao & Li, 2014):

$$C_l^{BB, \text{obs}} = C_l^{EE} \sin^2(2\alpha). \quad (11)$$

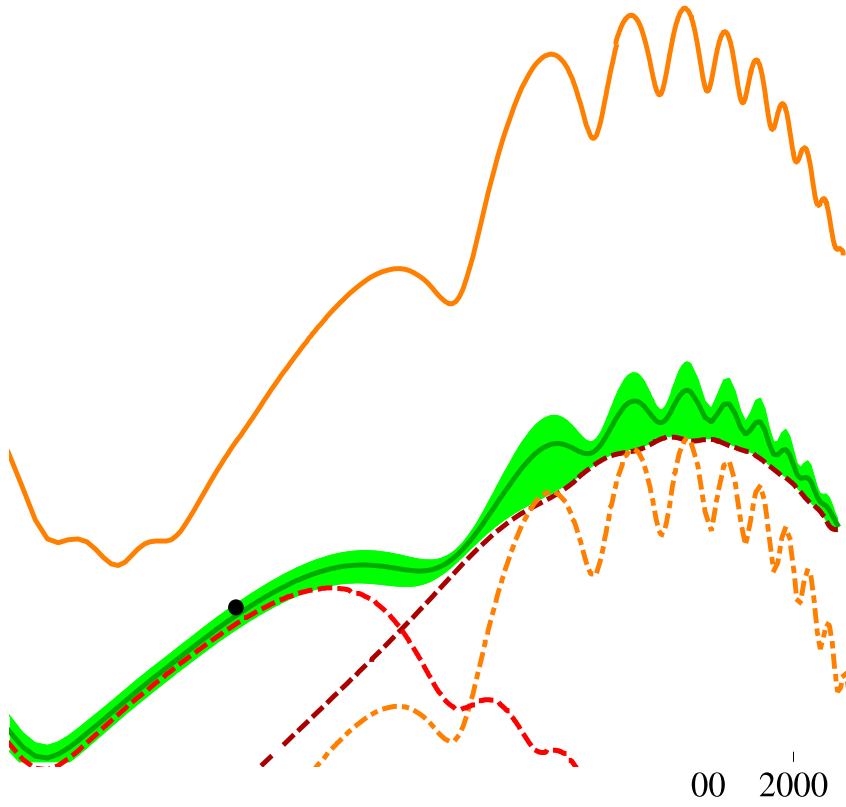
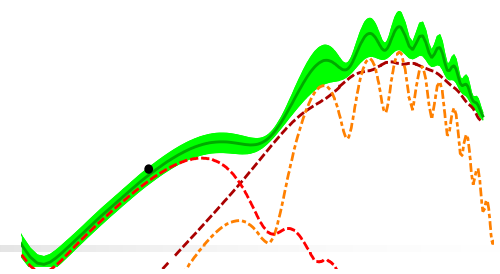
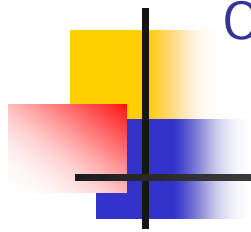
SPTpol results

- If the B-mode from the CPR propagation effect due to the pseudoscalar-photon interaction is correlated with the matter distribution, the correlation detection of SPTpol experiment would include this contribution.
- If that is so, we can further constrain the parameter $\alpha\eta$ since the tensor B-mode decreases quickly for $l > 500$. In our fits we assume 0%, 16.7%, 42.5%, and 100% correlation of the contribution from the cosmic polarization rotation to the power spectra depending on the dynamical model of pseudoscalar considered.



NEW CONSTRAINTS ON COSMIC POLARIZATION ROTATION FROM DETECTIONS OF B-MODE POLARIZATION IN CMB

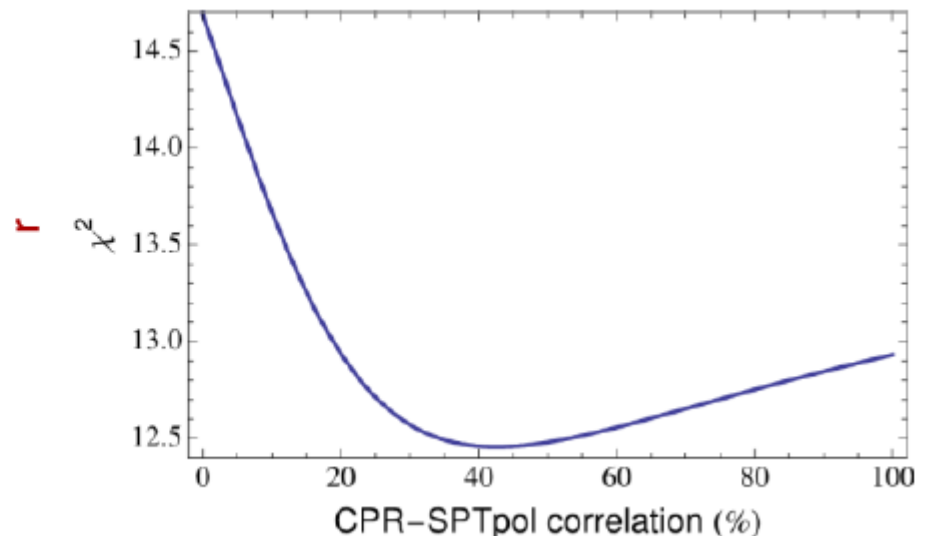
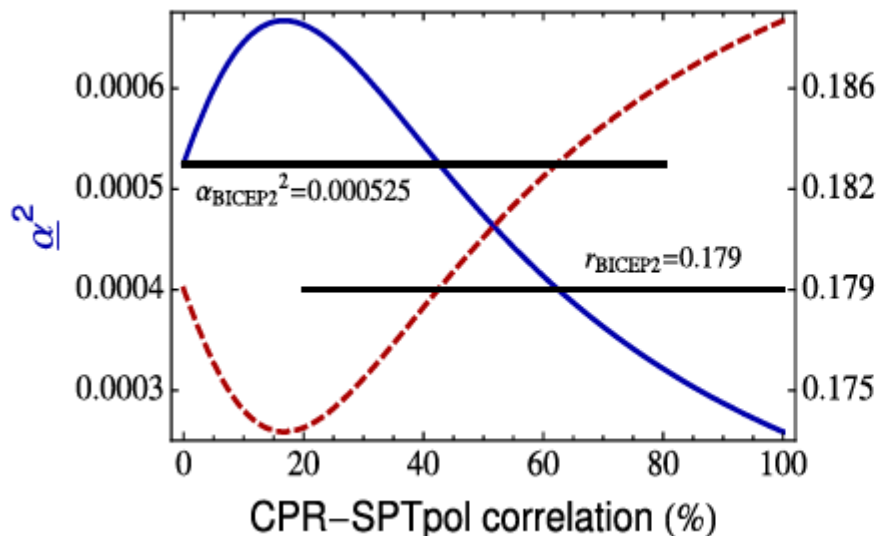
Alighieri, Ni and Pan



Tensor B ($r = 0.188$)

CPR fitting to BICEP2 & SPTpol

- Our fits give $r = 0.18 \pm 0.03$ and $\alpha_\eta^2 = \eta^2 \langle a \rangle^2 + \langle \delta a^2 \rangle = 0.000667 \pm 0.00052$, where $(1-\eta)$ is the efficiency in the uniform angle de-rotation, which is sometime applied to the measured CMB Q and U maps to compensate for insufficient calibrations of the polarization angle (Keating et al. 2013).
- This value of α_η^2 results in an upper limit $\alpha_\eta < 0.0345$ rad (1.97°).





Discussions (1404.1701)

- we have investigated, both theoretically and experimentally, the possibility to detect CPR, or set new constraints to it, using its coupling with the B-mode power spectra of the CMB.
- Three experiments have detected B-mode polarization in the CMB:
 - SPTpol (Hanson et al. 2013) for $500 < l < 2700$,
 - BICEP2 (Ade et al. 2014b) for $20 < l < 340$, and
 - POLARBEAR (Ade et al. 2014c) for $500 < l < 2100$.



Two Issues in practical realization

- First, in order to eliminate the observed excess of TB and EB power over the lensing expectations, the BICEP2 and the POLARBEAR collaborations have applied a de-rotation of $\sim 1^\circ$ to the final Q/U maps by minimizing the TB and EB power, since they cannot calibrate the overall polarization angle at this level of accuracy (Kaufman et al. 2014).
- By minimizing the TB power, the mean pseudoscalar polarization rotation angle is de-rotated by 2α and only the fluctuation part remains included in the BB polarization spectra. Minimizing EB power, the mean pseudoscalar polarization rotation angle is also de-rotated by about 2α . So the constraint on α is on the fluctuations and the leftover α of φ to the precision of rotation.



Two Issues in practical realization

- The SPTpol collaboration have not explicitly de-rotated their polarization data, but state that, although they have corrected for leakage of the CMB temperature into polarization ($I \rightarrow Q$ and U), the effect of this correction on the measured polarization amplitude is less than 0.1σ (Hanson et al. 2013).
- They also state that their systematic uncertainty on the polarization angle is less than 1° at 150 GHz.

Possible contamination of B-mode power spectra due to foreground anisotropies

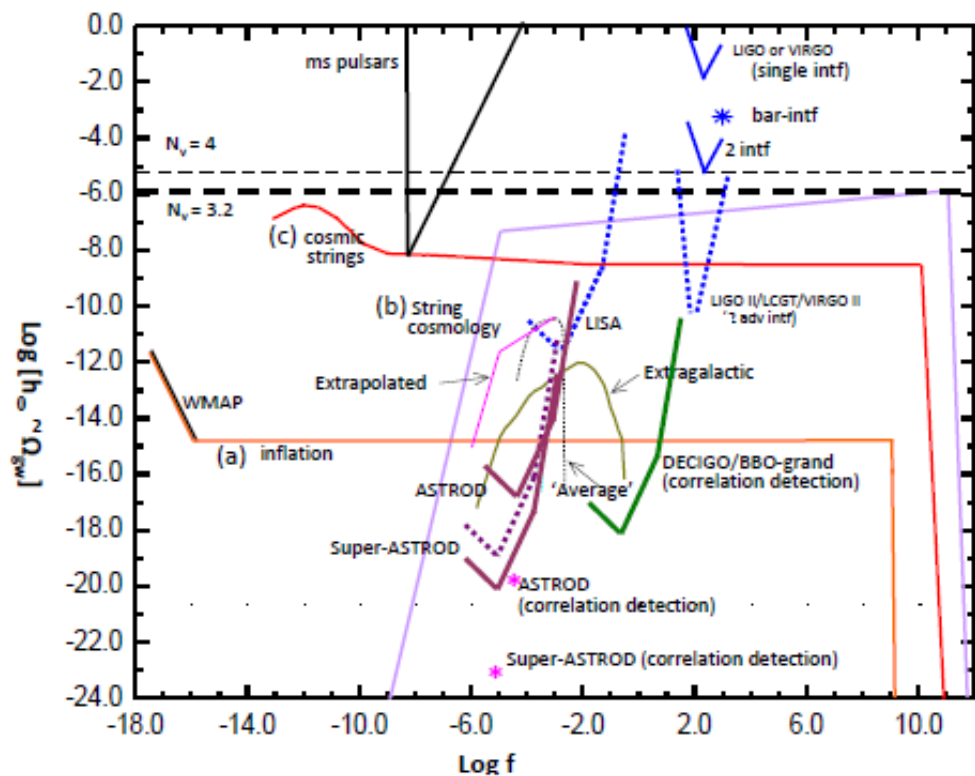
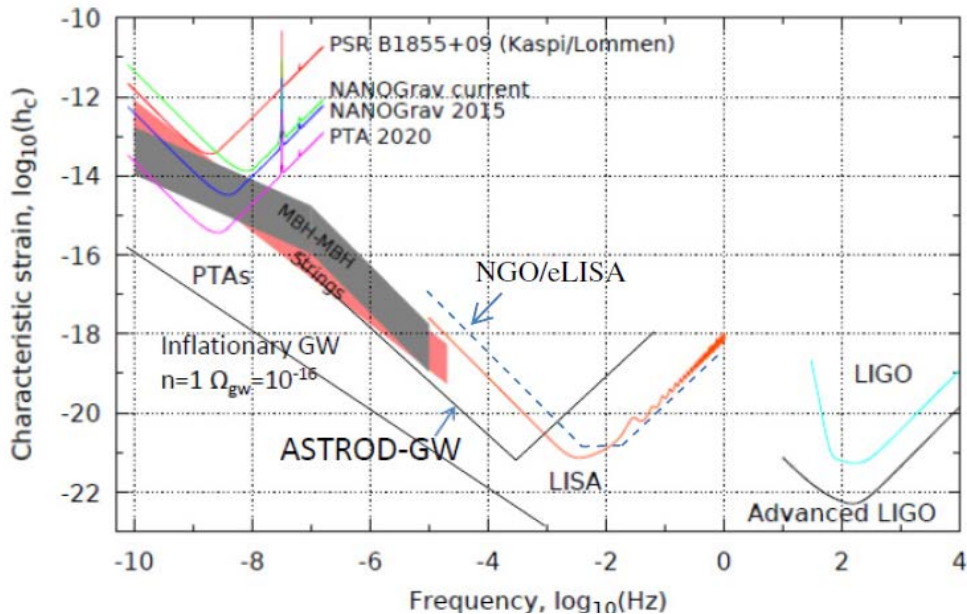
- The second practical issue is related to : the galactic ones are minimized by a careful selection of the observed sky regions, while those due to **distant FIR-luminous galaxies** can have **an effect at $l > 500$** (e.g. Holder et al. 2013).
- However, **the SPTpol team has applied a correction derived from Herschel data** (Hanson et al. 2013). On the other hand the POLARBEAR collaboration finds that the foreground contamination is negligible and have not corrected for it (Ade et al. 2014c).
- We notice that **the POLARBEAR data on CBB at $l=700$ (the only one with $S/N > 1.5$), which is not corrected for foreground contamination, is consistent with the higher S/N SPTpol data, which have been corrected**, giving us some confidence that the correction should not have an adverse influence.

Outlook

- 100 GHz Keck Array data will be available soon
- Three frequency BICEP3/Keck Array data (coming 2015?), should be able to characterize foregrounds
- Planck will soon release its polarization data which will be extremely valuable for our understanding of foregrounds because of its frequency coverage
- If pseudoscalar-photon interaction exists, a natural cosmic variation of the pseudoscalar field at the decoupling era is 10^{-5} fractionally. The CPR fluctuation is then of the order of $10^{-5}\phi_{\text{decoupling-era}}$. We will look for its possibility of detection or more constraints in future experiments.
- Next generation missions would be able to probe this

Primordial Gravitational Waves

- strain sensitivity
- →
- (ω^2) energy sensitivity
- Ω : energy sensitivity in terms of cosmic closure density



Primordial GW detection in space 2035+

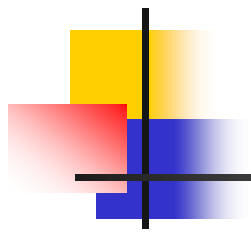


- eLISA is planned for Launch in 2034. Assume 1-year transfer to science orbit configuration, observation could start in 2035
- Large r makes the possible detection of primordial GWs realistic. After 2035, proposals like ASTROD-GW, BBO and DECIGO have chances to be implemented.



Summary

- CPR is a way to probe pseudoscalar-photon interaction and a way to probe inflation dynamics, especially in view of a possible high r
- New CPR constraints from B-mode are explored
- De-rotation is a way to measure CPR with calibration accuracy
- CPR is a means to test EEP or to find new physics
- From the empirical route to construct spacetime structure, axion and type II skewon are possibilities which could be explored further



Thank You !